CHARACTERIZING FUNCTIONALLY GRADED METALLIC ALUMINUM FOAMS BY MEANS OF THE INFILTRATION METHOD IN SOLUBLE PREFORMS AND THEIR APPLICATION IN PROGRAMMED DEFORMATION ELEMENTS

Patricio Abarca Pérez
edison.abarca@espoch.edu.ec
Escuela Superior Politécnica de Chimborazo
0000-0001-7041-4805
Fabián Sánchez Carrión
esanchez_c@espoch.edu.ec
Escuela Superior Politécnica de Chimborazo
0000-0002-8027-2799
David Bravo Morocho
victor.bravo@espoch.edu.ec
Escuela Superior Politécnica de Chimborazo
0000-0001-5629-259X
José Rodríguez Guambo
jr1@hotmail.com
Escuela Superior Politécnica de Chimborazo

Abstract

The study was carried out under an experimental protocol for obtaining metallic aluminum foams with varied porosity. The protocol was based on the infiltration method in water-soluble preforms; sodium oxide (Na2O) was used as preform material, with sizes of 3, 5 and 7 mm respectively, which were placed in a pyramid shape. A metallographic analysis was carried out to determine the most relevant properties of the metallic foams, such as relative density, porosity and bond thickness. As a result of this analysis, an average relative density of the foams of 0.504 and an average porosity percentage of 49.578% were obtained. To know the ligament thickness, the Image J computer program was used, and a thickness of approximately 0.94, 1.5 and 1.8 mm was obtained for pore diameters of 3, 5 and 7 mm, respectively. As part of this research, quasi-static compression testing was performed to obtain the energy absorbed by integrating the area under the stress-strain curve. To complete the mechanical test, a dynamic compression test was carried out by frontal impact of a pendulum designed for automotive applications, in order to observe the behavior of the foams as shock absorbers. Finally, the energy absorbed was studied by calculation and demonstrates the great capacity of this type of foams to absorb deformation energy.

Keywords: Metallographic, Metallic foams, Porosity, Impact absorbers, Quasi-static test.

1. Introduction

The research study refers to the manufacture of metallic aluminum foams, for which the method of infiltration in soluble preforms was considered, for being the most suitable and easy to use in our

environment. For the preform, sodium oxide was used with diameters of 3, 5 and 7 mm respectively and stacked in the form of a pyramid inside a cylindrical mold.

The purpose of the study is to analyze and describe the foam manufacturing processes in the country and its use. In the central zone of the country, such as the cities of Riobamba and Ambato, there are bodywork companies, which are potential markets for the application of metallic foams as impact absorbers. When talking about safety when getting into a vehicle, airback and bodywork almost always come to mind, but not the passive safety elements. These elements are always evolving and their function is to minimize the damage caused by a crash or impact to the driver and passengers.

Aluminum is widely used to manufacture this type of foams since it is an easily accessible and low-cost material. It has excellent physical and mechanical characteristics, such as resistance to weight ratio, low density, low melting point that can be reached with the infiltration method. In addition, recycled aluminum can be used to contribute to and promote a healthy environment free of waste that can affect the environment. The process that was implemented was based on studies carried out abroad and adjusted to the environment. The foams were subjected to a metallographic analysis to determine their most important properties such as relative density, porosity, pore size and pore ligament thickness. After this, mechanical compression and impact tests were performed.

Finally, a study was made of the results of both the compression test and the impact test, comparing them with similar foams obtained in previous studies.

2. Objectives

2.1 General Objective

To obtain and characterize functionally graded aluminum metal foams by means of the infiltration method in soluble preforms and their application in programmed deformation zones.

2.2 Specific objectives

- To select and assemble the equipment elements to obtain functionally graded open cell aluminum metal foams.
- To obtain functionally graded open-cell aluminum metal foams by the method of infiltration of molten metal into soluble or removable preforms.
- To mechanically and morphologically characterize the functionally graded open-cell aluminum metal foams obtained.

3. Hypothesis

Will the infiltration method allow to obtain functionally graded aluminum metal foams in soluble preforms and their application in shock absorbers?

4. Experimental methodology

The main objective of the research is the fabrication and characterization of functionally graded aluminum metal foams with open pore by the infiltration method in soluble preforms. For this purpose, the feasibility of the method was compared to other methods.

4.1 Feasibility analysis of the infiltration method for the manufacturing process

For the feasibility analysis of the study, the costs were analyzed, as well as accessibility to the technology for the manufacture of foams, and with the lowest investment cost, which is shown in Table 1.

PROCESS	TECHNOLOGY		COST OF PROCESSING		FOAM QUALITY		
	FACTIBLE	NOT FACTUAL	ALTO	UNDER	ALTA	MEDIA	BAJA
Gas injection into molten metal (HYDRO/CYMAT)		x	x			x	
Addition of foaming agent to molten metal (Alporas)	x		x		X		
Infiltration of molten metal into soluble preforms	x			x		x	
Casting using a polymer or wax precursor as a mold	x		x		X		
Powder Metallurgy	x		x			x	

Table 1: Feasibility of the infiltration process in relation to others

Source: Own elaboration

As shown in Table 1, the process by means of infiltration in soluble preforms is the most feasible due to the accessibility of the materials and at an acceptable cost.

4.2 Experimental methodology flowchart

The experimental methodology for the fabrication was based on the work of (Elizondo Luna et al., 2014), for the preparation of the sample and necessary equipment. For them, the flow diagram of the whole research process was considered as can be observed in Figure 1.

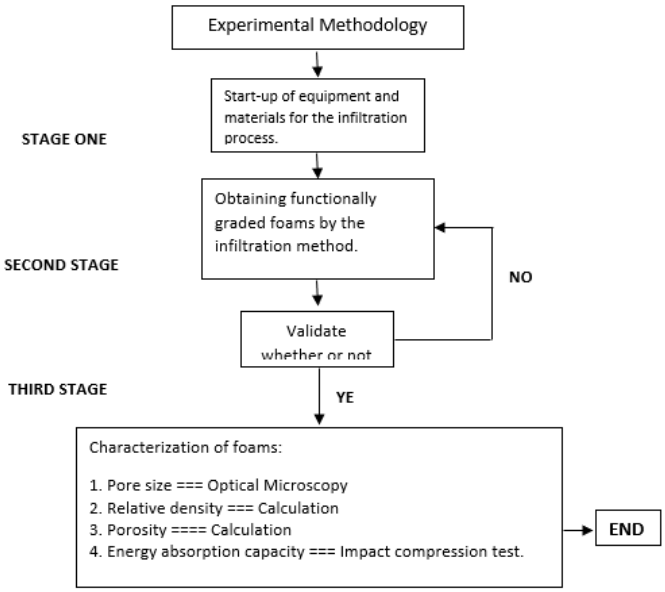

Figure 1: Flow chart for experimental methodology

Source: Own elaboration

4.3 Materials and equipment used

4.3.1 Soluble preform

The water-soluble preform material to be used is sodium oxide (Na2O), which will be sieved according to the desired pore size. For the research, sizes 3, 5 and 7 mm, are used. The characteristics of sodium oxide are presented in Table 2.

Formula	Na_2 O
Molecular weight	61.97 gr/mol
Appearance	Yellow crystalline solid
Melting point	1 132°C
Boiling point	1950 °C
Density	2.27 gr/cm^3
Solubility in H_2 O	YES

Table 2: Properties of sodium oxide.
Source: (Diaz, 2020)

Figure 2: Sodium oxide preform
Source: Own elaboration.

4.3.2 Base metal for infiltration

Aluminum is an excellent material for infiltration by this method, both for its physical and mechanical characteristics. With a melting point of approximately 660°C, which is relatively lower than that of sodium oxide at 1132°C, it can be infiltrated through the preform and then dissolved.

4.3.3 Aluminum melting furnace

The furnace used is of the crucible type, which will allow obtaining the aluminum billet or cylindrical bar, which will later be machined on a lathe to be introduced into the cylindrical mold. The furnace is located in the foundry laboratory of the faculty of mechanics.

4.3.4 Cylindrical mold for casting

Figure 2 shows the casting mold scheme, which consists of a cylinder, an upper cover (which connects to the valve system) and a lower cover, each with a groove for coupling to the cylinder, which will be fixed by bolts to prevent temperature convection at the time of casting (Elizondo Luna et al., 2014)

The mold shall be made of stainless steel, in order to avoid corrosion when working at high temperatures.

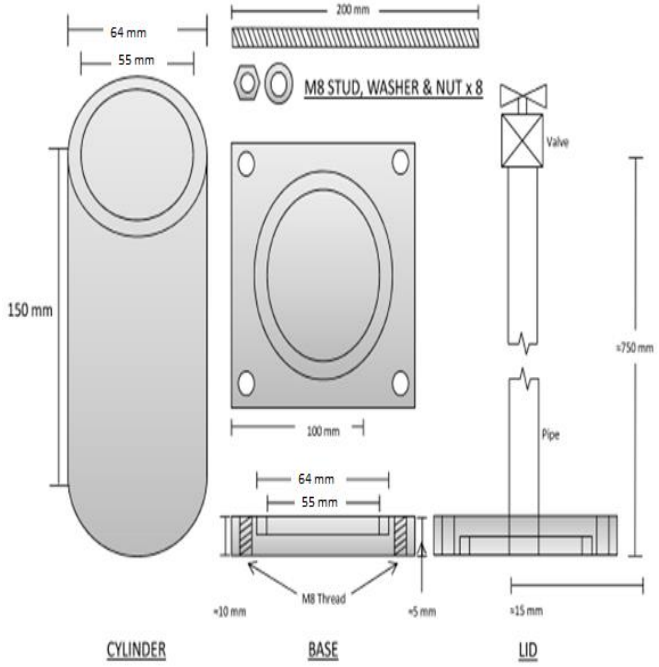

Figure 2: Mold for casting of aluminum foams
Source: Elizondo Luna et al. (2014)

4.3.5 Electric furnace for the manufacture of foams

The most important variables of the process are temperature and melting time, because the aluminum billet must reach the right temperature to infiltrate the entire preform into the stainless-steel cylinder. A muffle furnace with digital temperature control will be used.

Description	***Detail***
Internal dimensions	23x18x18 cm
External dimensions	35x30x30 cm
Material inner chamber	High alumina refractory bricks (withstands up to 1400°C)
Maximum working temperature	1200°C
Continuous working temperature	1100°C
Voltage	220 V
Amperage	15 A
Power	3300 W
Number of phases	1

Thermocouple	Type K with ceramic coating
Temperature controller	Model K

Table 3: Electric muffle furnace characteristics
Source: Own elaboration

Figure 3: Electric muffle furnace
Source: Own elaboration

4.3.6 Vacuum pump

To prevent the aluminum from reacting with oxygen, a vacuum is created inside the cylindrical mold by means of a pump, which is also fitted with a vacuum gauge to measure the level of vacuum created. Table 4 shows the characteristics of the vacuum pump.

Figure 4: Vacuum pump
Source: Own elaboration

Model	QVP-800
Voltage	110 V/ 60 Hz
Power	¾ HP
Ultimate vacuum	3 x10^{-1} Pa
Oil capacity	600 ml
Free air displacement	8.0 CFM

Table 4: Vacuum pump technical characteristics
Source: Own elaboration

4.3.7 Argon tank

Argon is a noble gas that does not react with other elements, so it will be used to generate a positive pressure inside the cylindrical mold. The capacity of the tank is 6 m3.

Figure 5: Argon tank
Source: Own elaboration

4.3.8 Graphite

Graphite as a foil will be used as a thermal insulator and as powder particles to prevent corrosion of the aluminum with the walls of the cylindrical mold.

Figure 6: Powdered graphite and foil
Source: Own elaboration

4.3.9 Sieves

To generate preforms of 3, 5 and 7 mm diameter, the sodium oxide will be sieved by placing sieves of the desired range one below the other in descending order.

Figure 7: Sieves sorted by pore diameter
Source: Own elaboration

4.3.10 Mechanical sieve shaker

The mechanical stirrer will be used to move the ordered sieves for a certain period of time to achieve the amount of sodium oxide needed to generate the aluminum foam samples.

Figure 8: Mechanical sieve shaker
Source: Own elaboration

4.3.11 Pyrometer

For temperature control inside the cylindrical mold, the pyrometer is used, since the temperature is not the same in the furnace as inside the cylinder, so it is iterated by programming several temperature cycles in the electric furnace. The pyrometer will check the temperature of a replica mold in order to achieve the proper infiltration temperature.

4.4 Equipment schematic for infiltration process

As shown in Figure 9, the scheme consists of: vacuum pump, argon tank, electric furnace, and the valve system that allows the flow of argon into the interior; and in the same way, to extract the oxygen inside the cylinder chamber to the outside, in order to create an almost ideal environment for casting.

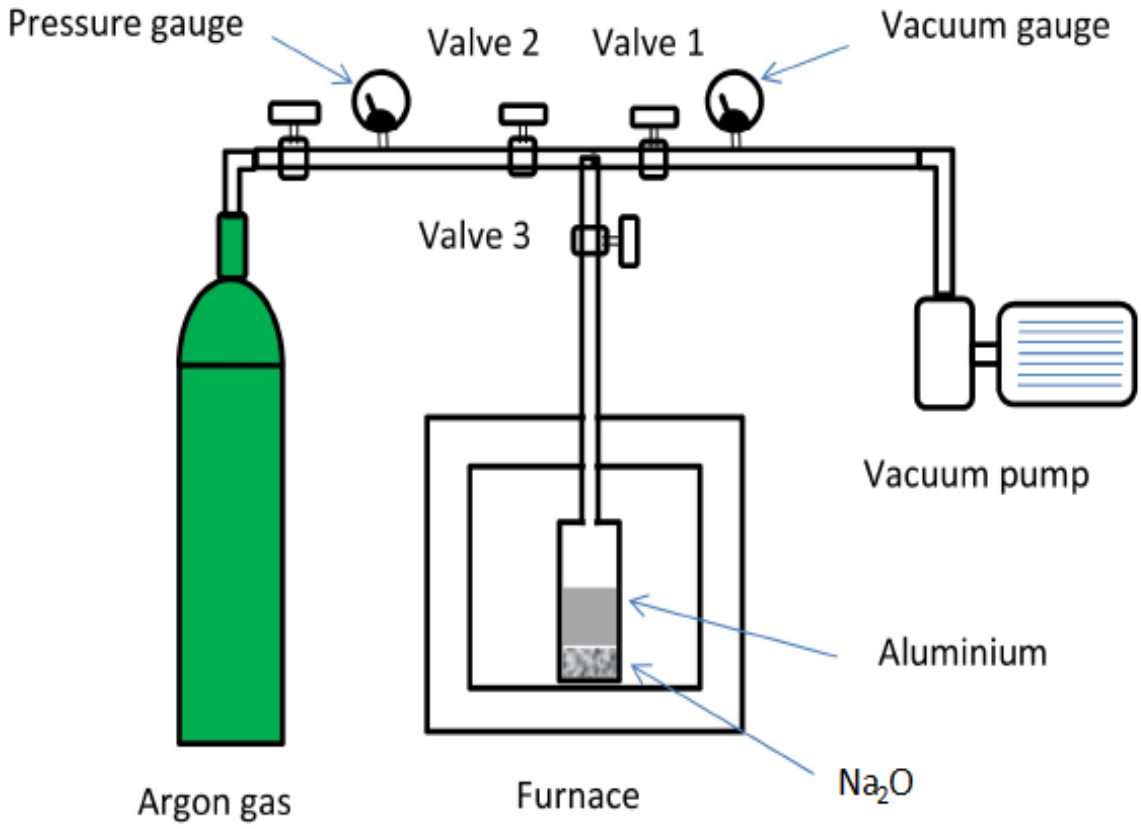

Figure 9: Schematic diagram of the equipment for the infiltration process.
Source: Elizondo Lunaet al. (2014)

4.5 Experimentation

4.5.1 Manufacture of cylindrical molds

The cylindrical mold was machined in accordance with the dimensions established in section 3.3.4. The mold consists of:

- Four through bolts (a)
- Cylinder (b)
- Four nuts (c)
- Upper and lower cover (d)

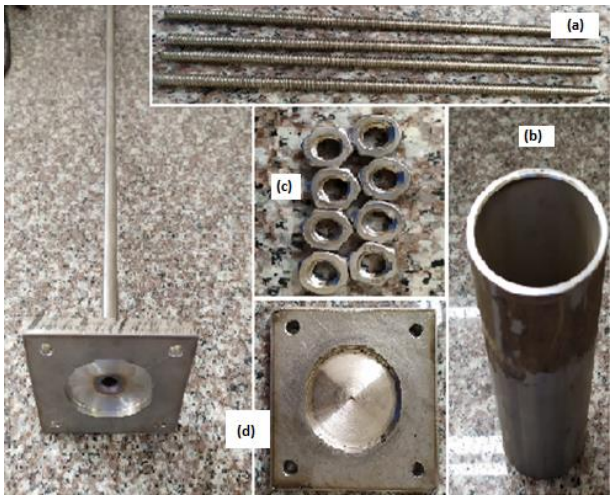

Figure 9: Cylindrical Mold
Source: Own elaboration

4.5.2 Preparation of the aluminum billet

The following steps were followed to obtain the aluminum billets:

a. Prepare the sand mold
b. Turn on the crucible oven and place the aluminum until it is completely melted (Approximately 1h).
c. Pour the molten aluminum into the sand mold.
d. Wait until completely cooled and remove the aluminum billet.
e. Machining the aluminum billet to a diameter of 55 mm.

Figure 10: Machined aluminum billet
Source: Own elaboration

4.5.3 Oven preparation

Set a temperature of 340°C in the oven for approximately 2 hours, sufficient time to preheat the oven adequately. In addition, the oven speed should be set at 20°/min, to reach the optimum temperature so that the molten aluminum can infiltrate inside the preform (Abarca, 2017).

4.5.4 Preform preparation

The preparation of sodium oxide as a preform material is detailed below:

a. Select the size of sodium oxide (3.5 and 7 mm) and the amount needed to generate the samples.
b. A mechanical stirrer is used to sieve the required amount according to the pore size.

c. Place the preform according to size, in plastic containers.

Figure 11: Sifting and packing of sodium oxide

Source: Own elaboration.

4.5.5 Mold preparation

a. Clean the mold of any impurities

b. Place a thin layer of powdered graphite inside the cylinder in order to prevent adhesion of the molten aluminum.

c. Place a sheet of graphite on the bottom and top covers to generate the necessary insulation.

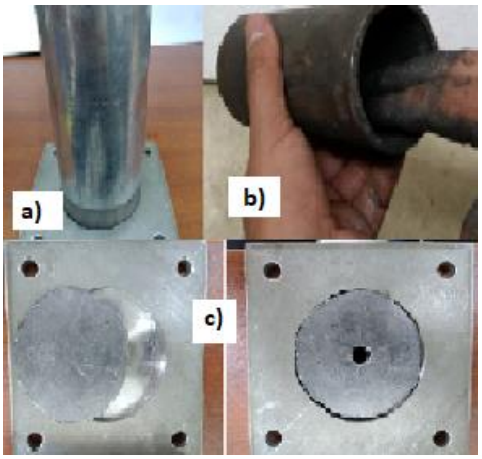

Figure 12: Cleaning and isolation of the cylinder by graphite

Source: Own elaboration.

d. Assemble the cylinder by means of the studs and the bottom cap.

e. Stack the spheres of sodium oxides in a pyramid shape to get the graduated preform.

Figure 13: Cylinder assembly and preform placement
Source: Own elaboration.

f. Place the aluminum billet on the preform inside the cylindrical mold, and insulate by means of the upper cover so that it is completely sealed.

Figure 14: Fully hermetized mold
Source: Own elaboration.

g. Preheat the muffle furnace. Place the replica mold inside the furnace and with the help of the pyrometer control the temperature until it stabilizes. To achieve good infiltration results, the replica cylinder should be stabilized at a temperature of 800°C.
h. Fasten the upper part of the cover with the valve system, by means of a union nut.

Figure 15: Attachment of the valve system to the mold.
Source: Own elaboration.

i. Close all valves in the system
j. Open the valve leading to the vacuum pump and the mold (valve 3).

k. Turn on the vacuum pump until the gauge on the valve system reads the lowest possible pressure.

l. Turn off the vacuum pump.

m. If the vacuum loss in the system is less than a range of 50 torr/s during the first 10 seconds after turning off the vacuum pump, the seal is good enough for infiltration to occur.

n. Leave the valve on the lid open (valve 3) to keep the system at ambient pressure and close the valve on the vacuum pump (valve 1).

o. Without disassembling the valve system, place the mold in the preheated oven and wait 1

4.5.6 Infiltration

a. Close the system valves.
b. Open the conductive valve to the argon gas cylinder.
c. Open the main valve of the argon gas tank with a pressure of approximately 3.5 bar (Elizondo Luna et al., 2014).
d. Quickly open valve 3.
e. Wait 1 hour, remove the mold from the oven and place it on a metallic surface (copper recommendation) in order to allow the heat flow to dissipate to the outside. In this process the cooling pressure will vary a little, so it should be regulated to the initial pressure if necessary.

4.5.7 Sample Extraction

a. After approximately 30 min, the mold is sufficiently manipulable to uncouple valve 3 from the system and unscrew the upper mold cover.
b. Remove the cylinder completely and place it in a hand net.
c. Using a rubber hammer tap the back of the foam to remove the foam from the cylinder.
c. Using a band saw cut the excess aluminum from the bottom of the foam.
d. Depending on the height of the foam required, cut off the top of the sample.
e. Place the sample in a container with water in order to remove the sodium oxide. To carry out a periodic change of water when its temperature oscillates the 60°C, every ten minutes.
f. Once the sodium oxide has been completely removed, the sample is dried with air from the compressor.

5. Results

This section shows the structural and mechanical characterization of the foams, which are the objectives of our research.

5.1 Structural characterization

The characterization of foams is based on knowing their cellular topology, as well as their relative density, shape and pore size.

5.1.1 Microstructure and hardness of aluminum foam

Microstructure

In order to know the microstructure of the aluminum foams, a sample was taken and based on ASTM E3 (Standard guide for the preparation of metallographic samples) and ASTM E407 (Chemical attack. Standard practice for metals and alloys), the sample was prepared and then taken to the optical microscope. This analysis was carried out at the Metallographic Analysis Laboratory of the Centro de Fomento Productivo Metalmecánico Carrocero (CFPMC) of the Tungurahua Provincial Government.

Figure 16: OLYMPUS metallographic microscope
Source: Own elaboration.

Equipment used	OLYMPUS® metallographic microscope
Model	BX41M-LED
Series	4A42787
Attack time	15 seconds

Table 5: General metallographic test data
Source: Own elaboration

The images taken were as follows:

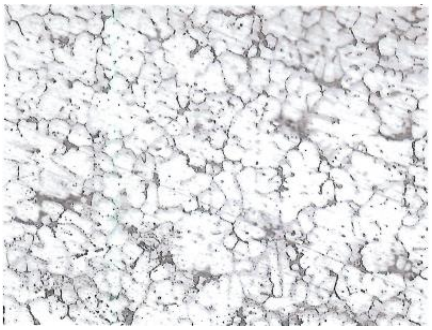

Figure 17. Microstructure magnified at 100X, Hydrofluoric acid, 15 **sec.**
Source: Own elaboration.

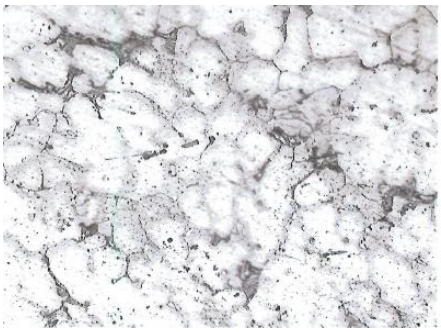

Figure 18. Microstructure magnified at 200X, Hydrofluoric acid, 15 **sec.**
Source: Own elaboration.

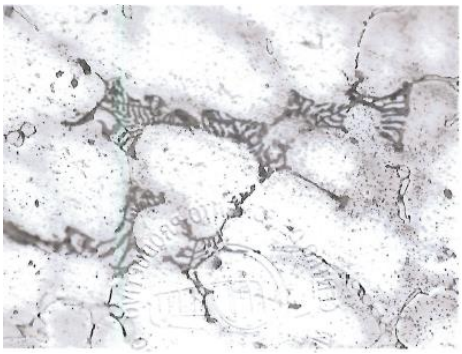

Figure 19. Microstructure magnified at 200X, Hydrofluoric acid, 15 **sec.**
Source: Own elaboration.

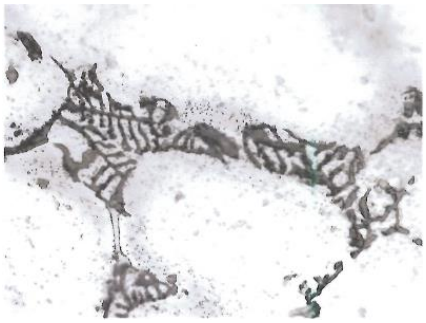

Figure 20. Magnified microstructure at 1000X, Hydrofluoric acid, 15 sec.
Source: Own elaboration.

Vickers hardness

To determine the hardness of aluminum foams, the Vickers microhardness test has been considered. For this purpose, a specimen is selected, the general data of the test are shown below.

Test method	NTE INEN-ISO 6507-1 Metallic materials
Type of test	Vickers hardness test
Type of test	Quantitative
Equipment used	FUTURE TECH micro-hardness tester
Model	FM 800
Series	FMX 8340

Force application time	15 seconds
Applied force	9.807 N
Last machine check	2020/10/28
Pattern Used	FT13159609
Value	699.3 HV1
Machine Verification By means of pattern	699.1 HV1

Table 6: General data of Vickers hardness test on aluminum foam.
Source: Own elaboration

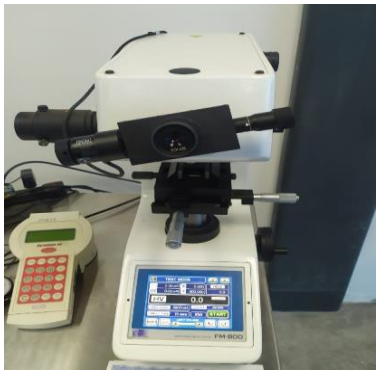

Figure 21: Future-Tech® Mycro-durometer
Source: Own elaboration.

The result obtained from the microhardness test is shown below in Table 7.

Probe	Identification	Temperature (°C)	Relative Humidity (%)	VICKERS hardness (HV1)		
				Diagonal 1 (μm)	Diagonal 2 (μm)	Hardness
1	EDV-01	23.2	51.7	160.01	159.69	72.6

Table 7: VICKERS microhardness in aluminum foam
Source: Own elaboration

5.2 Energy absorption capacity

The compression and impact tests were carried out at the facilities of the CENTRO DE FOMENTO PRODUCIVO METALMECANICO CARROCERO (CFPMC) of the H. Gobierno Provincial de Tungurahua located in the city of Ambato.

5.2.1 Uniaxial compression test

For the uniaxial compression test, two specimens were considered, which were coded according to the laboratory. The test was performed in a universal machine. The characteristics of the universal machine are presented in Table 8.

Team	Metrotest Universal Machine
Model	STH-1500 S/C
Series	8802M001

Table 8. VICKERS microhardness in aluminum foam
Source: Own elaboration

Figure 22. Metrotest Universal Machine
Source: Own elaboration.

Table 9 shows the general data with which the tests were carried out.

Place of execution of the test	Strength of Materials Laboratory
Address	Ambato / Catiglata. Toronto Ave. and Rio de Janeiro Ave.
Test method	Non-standardized
Type of test	Quantitative
Probe Type	Cylindrical
Material	Graduated aluminum foam
Number of test tubes	
Group Identification	ECM 01
Test speed	10 mm/min
Preload	1000 N
Trial start date	2020/04/22
Trial end date	2020/04/22

Table 9. General data of the compression test
Source: Own elaboration

Tables 10, 11 and 12 show the dimensions and results of forces, stresses and deformation of the specimens subjected to the uniaxial compression test.

Probe	Identification	Temperature (°C)	Relative Humidity (%)	Dimensions (mm)	
				Diameter	Length
1	ECM 01-1	19.3	58.3	54.54	61.59
	ECM 01-2	19.4	57.1	53.86	54.01

Table 10. Preliminary data and dimensions of compression specimens

Source: Own elaboration

c	Identification	Maximum strength (N)	Maximum Effort of Compression (MPa)	Displacement (mm)	% of maximum deformation
1	ECM 01-1	98 100.01	41.99	7.804	12.67
	ECM 01-2	40 000.00	17.56	3.776	6.99

Table 11. Force, Strain, Displacement and maximum deformation of specimens subjected to compression

Source: Own elaboration

Probe	Identification	Ultimate strength (N)	Ultimate effort of Compression (MPa)	Ultimate displacement (mm)	% ultimate deformation
1	ECM 01-1	75 700.01	32.40	20.512	33.30
	ECM 01-2	37 800.00	16.59	5.712	10.58

Table 12. Force, Stress, Displacement and ultimate strain of specimens subjected to compression.

Source: Own elaboration

Figure 23. Specimens prior to compression test

Source: Own elaboration.

The speed for the test was 10 mm/min and a preload of 1000 N, deforming as follows:

a. Application of preload
b. Deformation at a speed of 10 mm/min
c. Pore collapse

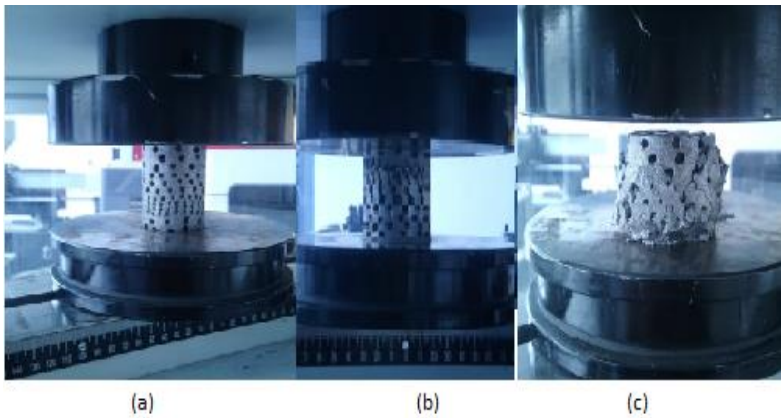

Figure 23. Specimens prior to compression test
Source: Own elaboration.

The universal machine offers the possibility of extracting the results of the compression test to be able to tabulate either in Excel or any other calculation program. In addition, it presents force and stress graphs in order to see the compression zones present in the foams.

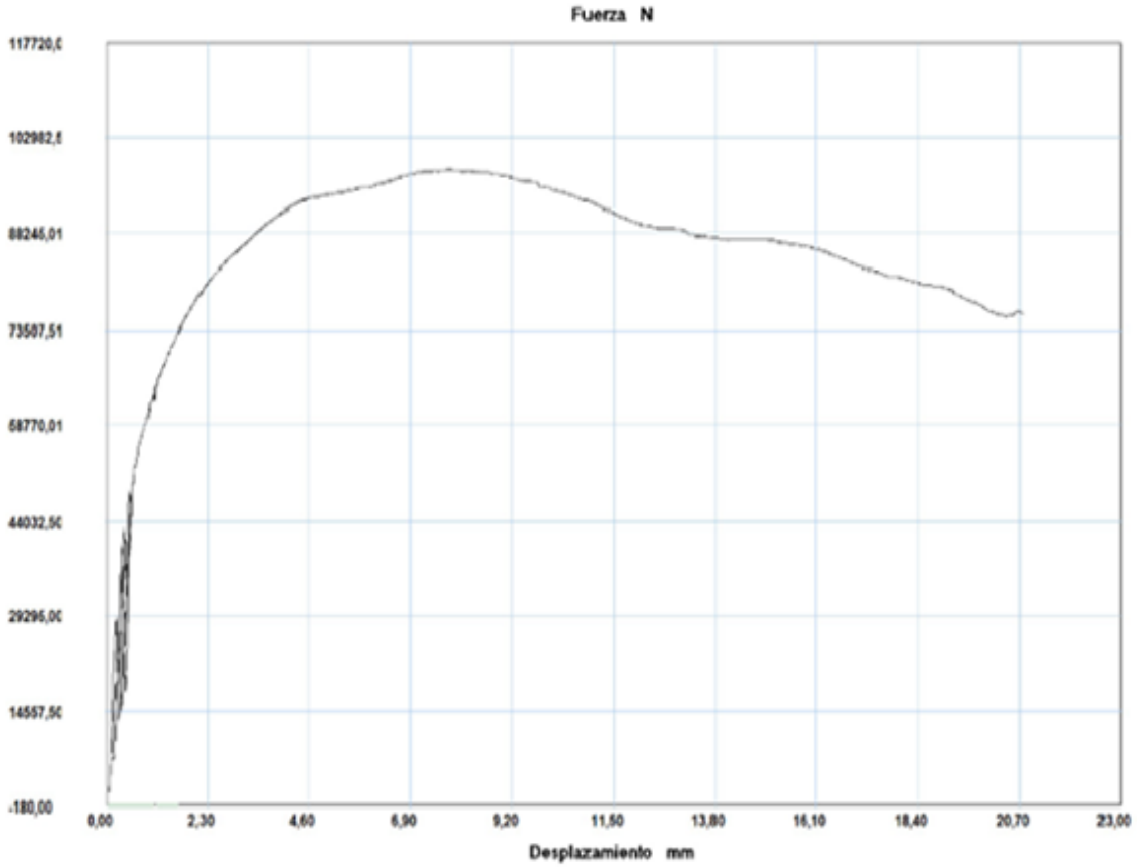

Figure 24. Force vs. displacement of specimen ECM 01-1
Source: Own elaboration.

Figure 25 shows the statistical parameters of the ECM-01-1 specimen subjected to compression.

Probeta	FMax N	CMax MPa
■ 1	98100,01	41,99
Media	98100,010	41,990
Mediana	98100,010	41,990
Desv. Std	0,000	0,000
Coef. V.	0,000	0,000
Máximo	98100,010	41,990
Mínimo	98100,010	41,990
Rango	0,000	0,000
CPK	0,000	0,000
+3 Sigma	98100,010	41,990
-3 Sigma	98100,010	41,990

Parametros

Precarga	=	1000,00	N
Caida %	=	100,00	
Retorno Automatico	=	0,00	
Limite Fuerza	=	1500000,00	N
Limite Desplazamiento	=	50,00	mm
Stop Ext	=	50,00	mm

Velocidades

Precarga	=	10,00	mm/min
Ensayo	=	10,00	mm/min
Retorno	=	50,00	mm/min
Posicionamiento	=	50,00	mm/min

Figure 24. Statistical parameters of the ECM-01-1 specimen subjected to compression.
Source: Own elaboration.

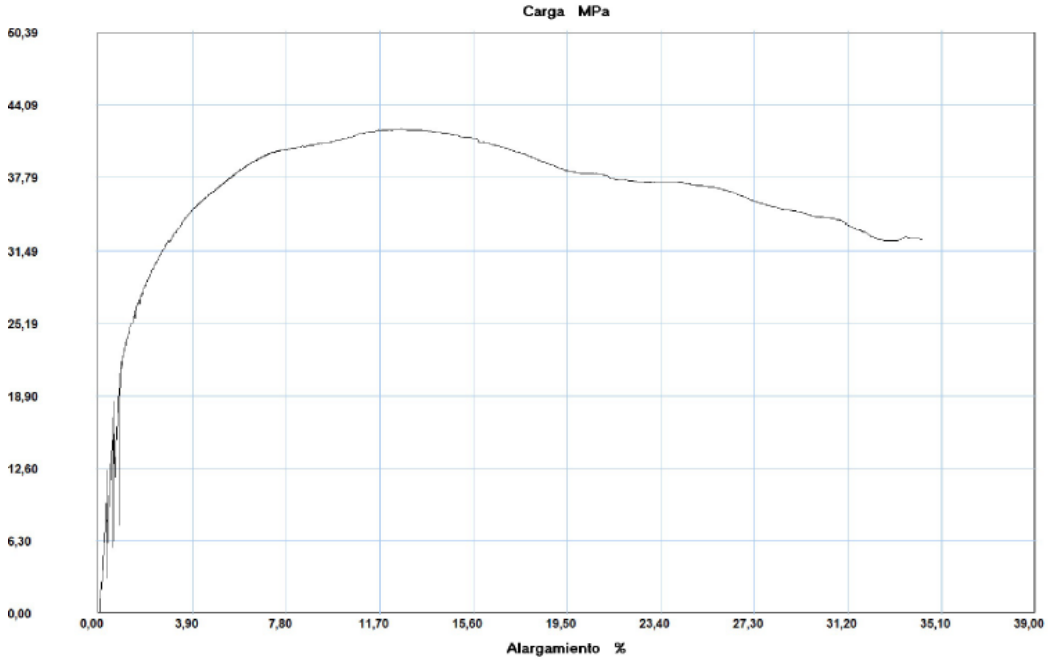

Figure 25. Load vs % displacement plot of ECM 01-1 specimen.
Source: Own elaboration.

Figures 26, 27 and 28 show the graphs and statistical data for specimen ECM 01-2 subjected to compression.

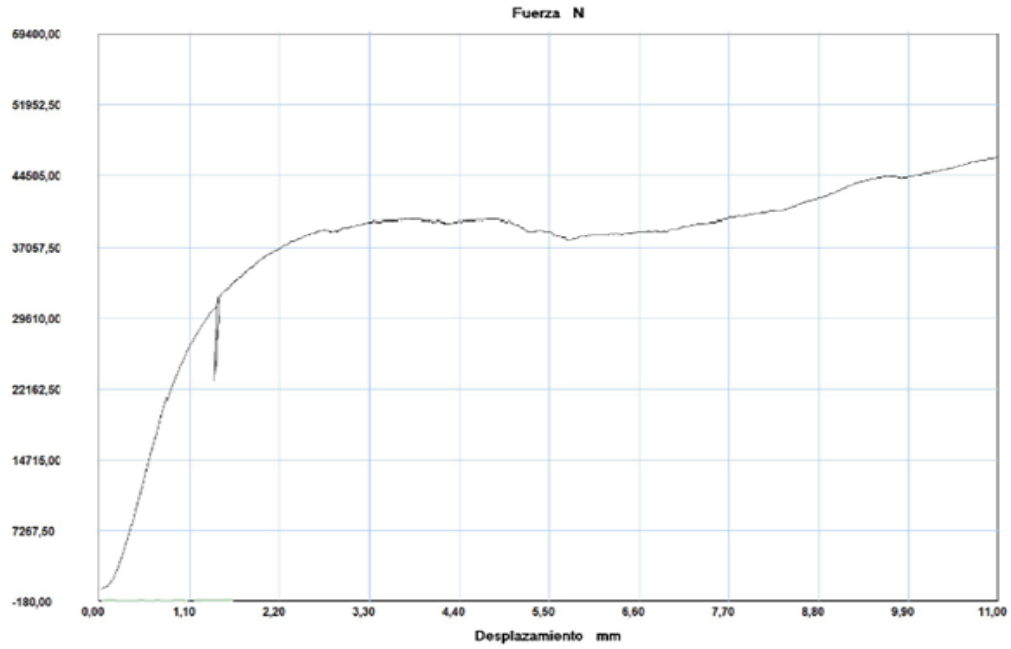

Figure 26. Force vs. displacement of specimen ECM 01-2
Source: Own elaboration.

Probeta	FMáx N	CMáx MPa
■ 2	40000,00	17,56
Media	40000,000	17,556
Mediana	40000,000	17,556
Desv. Std	0,000	0,000
Coef. V.	0,000	0,000
Máximo	40000,000	17,556
Mínimo	40000,000	17,556
Rango	0,000	0,000
CPK	0,000	0,000
+3 Sigma	40000,000	17,556
-3 Sigma	40000,000	17,556

Parametros			
Precarga	=	1000,00	N
Caida %	=	100,00	
Retorno Automatico	=	0,00	
Limite Fuerza	=	1500000,00	N
Limite Desplazamiento	=	50,00	mm
Stop Ext	=	50,00	mm

Velocidades			
Precarga	=	10,00	mm/min
Ensayo	=	10,00	mm/min
Retorno	=	50,00	mm/min
Posicionamiento	=	50,00	mm/min

Figure 27. Statistical parameters of the ECM-01-2 specimen subjected to compression.
Source: Own elaboration.

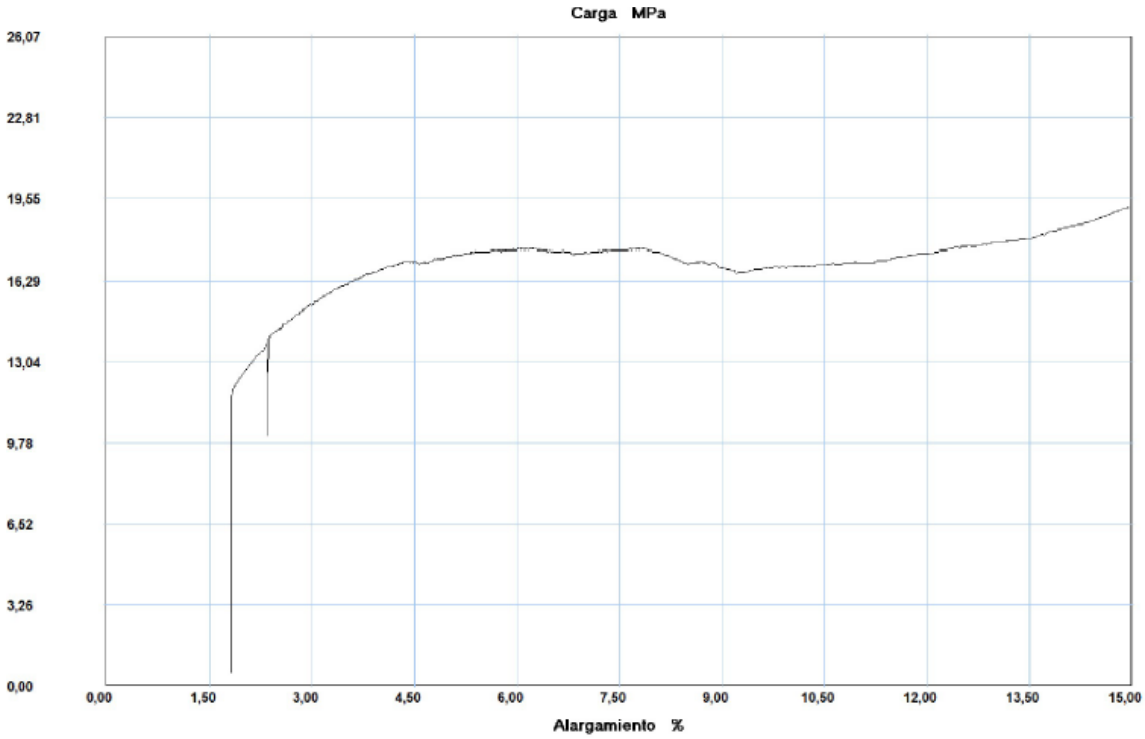

Figure 28. Load vs % displacement plot of ECM 01-2 specimen.
Source: Own elaboration.

6. Proposal

6.1 Application of functionally graded aluminum foams in shock absorbers

Table 13 summarizes the values of the impact energy generated by the four specimens tested by the Charpy test. On average, the energy absorbed was 15,085 J. It should be noted that the Charpy impact test is not established in any standard. Therefore, only the specimens were cut so that they could enter the housing to proceed with the test. The results shown in the research, specifically in the impact test, are purely investigative but not to issue or corroborate any information since there are no data on this test performed by other authors on aluminum foams for comparison (Illescas, 2009)

The severity of an accident is not linked to the speed of the vehicle before the collision, but by the change in speed Δv that the vehicle experiences and by the speed with which this change occurs, i.e., deceleration. The deceleration is determined by the mass and stiffness of the colliding objects (Illescas, 2009)

To bring the vehicle to a complete stop, the impact must dissipate all this energy. When the object hit is very rigid, such as a concrete barrier, all the energy must be absorbed by the vehicle. During the collision, deformation continues until all the energy involved in the accident is absorbed, i.e., until the kinetic energy is equal to the energy required to deform the structure.

To see if foams are suitable for use in impact absorbers, the mechanical properties are compared to a similar job, but with other types of aluminum foams.

Probe	Relative density	Porosity % Porosity	E (GPa)	σ_c (MPa)	σ_{pl} (MPa)	ϵ (%)
ECM-01-1	0.474	52.6		41.99		
ECM-01-2	0.389	0.611	0.6	17.56		
Alporas 10% Alporas 10% Alporas 10% Alporas 10% Alporas 10% Alporas 10% Alporas	0.1		0.17	1.9	2.2	

Table 13. Mechanical properties of functionally graded aluminum foams vs. Alporas 10%.
Source: Own elaboration

As can be seen in Table 13, the properties of the functionally graded foams ECM-01-1 and ECM-01-2 exceed those of the Alporas 10%, although the unit deformation of the Alporas foam is greater, which possibly has a greater absorption capacity due to the higher percentage of porosity. As we discussed in the compression test, the increase in mechanical properties is due to the size of the pore ligament, and also to the increase in precipitates that cause the hardening of the material.
Future work would be to improve the temperature control inside the cylinder during the casting of the aluminum foams, as well as to make a more rigorous analysis of the impact test, since our country does not have the necessary technology to perform a Crash Test, which allows measuring the efficiency of the foams inside any element of the vehicle structure.

6.2 Manufacturing costs

The costs shown in Table 14 include the cost of the elements for the assembly of the equipment for the manufacture of the aluminum foams, as well as the labor and logistics involved in its realization.

Material	Quantity	Unit Price	Total Price
Muffle furnace for metal smelting	1	1250	1250
Vacuum pump	1	275	275
Argon gas cylinder	1		
cylindrical mold	1	110	110
Valve system	1		
Graphite sheets			
Graphite powder			
Aluminum and Sodium Oxide			
Accessories			
Logistics			
		Total	$ 2 340

Table 14: Manufacturing cost.
Source: Own elaboration

7. Conclusions

- In the study, open-cell metallic aluminum foams were obtained by the water-soluble (sodium oxide) graded preform infiltration method, with grain sizes of 3, 5 and 7 mm, as shown in Figure 9-4.
- The foams obtained have an average relative density of 0.504, i.e., 49.578% porosity. This indicates that the percentage of porosity of the foams generated is slightly lower than that shown in other works. One of the reasons could be that larger diameter sizes were used.
- With respect to the structural characterization, a specimen was sectioned in order to observe and measure the pore size, using the Image J program. The pore diameter was measured in six regions, with an average value similar to that initially proposed (3, 5 and 7 mm). These values are shown in Table 5-4. In the same way, the thickness of the ligament between the pores was measured, giving an average ligament thickness of 0.94 mm, 1.49 mm and 1.69 mm for a pore size of 3, 5 and 7 mm respectively.
- Cylindrical specimens tested in uniaxial compression were found to have macroscopically ductile mechanical behavior consistent with that typically exhibited by similar foams.
- For the analysis of energy absorption, the values obtained in the uniaxial compression test were plotted. An approximate equation was obtained, which was integrated along the extended plateau region in order to find the energy absorbed by each of the specimens. It was found that, for the first specimen the energy was 28.67 J/m^3 and 2.84 J/m^3 for the second one. The difference in energy values is due to the fact that there was a hardening in one specimen, since it is difficult to control the temperature at the time of casting.

8. Recommendations

To see a better method of temperature control inside the cylindrical mold, and to avoid possible hardening effects by plastic deformation of the aluminum.

For future studies, see how to test the generated aluminum foams in order to prove their energy absorption already in vehicle safety elements, in order to verify and validate their efficiency.

References

Abarca, P. (2017). *Bibdigital*. Available at bibdigital.epn.edu.ec: http://bibdigital.epn.edu.ec/handle/15000/17431

Amir, H., Ali, H., & Hassan, B. (2012). *ScienceDirect.* Available at ScienceDirect: https://www.sciencedirect.com/science/article/abs/pii/S0261306912002671

Ashby, Evans, A. G., Fleck, N. A., Gibson, L. J., Hutchinson, J. W., & Wadley, H. (2002). *Espumas Metálicas. Una guía de diseño.* Johannesburg: Butterworth-Heinemann.

Avila, D., & Murias, D. (16 de 07 de 2016). *Circula Seguro*. Available at Circula Seguro: https://www.circulaseguro.com/las-zonas-deformacion-programada-coche-pueden-salvarnos-la-vida/

Cárcel, B. (Noviembre de 2015). *Universidad Politécnica de Valencia.* Available at Universidad Politécnica de Valencia:

https://riunet.upv.es/bitstream/handle/10251/61298/C%C3%A1rcel%20-%20Efectos%20de%20la%20estructura%20celular%20sobre%20el%20comportamiento%20mec%C3%A1nico%20de%20espumas%20de%20aluminio....pdf?sequence=1

Cerit, M., & Guler, M. (02 de 01 de 2010). *International LS-DYNA Users Conference*. Available at International LS-DYNA Users Conference: https://www.semanticscholar.org/paper/Improvement-of-the-Energy-Absorption-Capacity-of-an-Cerit-Guler/b805120ccf23437a631c1082a18e916b15681389

Diaz, R. (10 de 08 de 2020). *Lifeder*. Obtenido de Diaz, Rafael: https://www.lifeder.com/oxido-sodio/

Elizondo Luna, E., Barari, F., Woolley, R., & Russell, G. (11 de 12 de 2014). *Jove*. Available at Jove: https://www.jove.com/v/52268/casting-protocols-for-production-open-cell-aluminum-foams-replication

Fernandez, P., Cruz, L. J., & Coleto, J. (2008). Procesos de fabricación de metales celulares. Parte I: Procesos por vía líquida. *Revista de Metalurgia*, 540-555. Available at http://revistademetalurgia.revistas.csic.es/index.php/revistademetalurgia/article/view/142/140

Gutiérrez, J. A., & Oñoro, J. (2008). Espumas de aluminio. Fabricación, propiedades y aplicaciones. *Revista de Metalurgia*, 457-476. Available at https://www.researchgate.net/publication/44200232_Espumas_de_aluminio_Fabricacion_propiedades_y_aplicaciones/fulltext/0e609c04f0c44a2d53520d1e/Espumas-de-aluminio-Fabricacion-propiedades-y-aplicaciones.pdf

Hamza, O., Omran, A. M., Atlan, A. A., & Moatasem, M. K. (2017). CHARACTERIZATION OF ALUMINIUM FOAM PRODUCED FROM ALUMINIUM SCRAP BY USING CaCO3 AS FOAMING AGENT. *Journal of Engineering Sciences*, 448-459.

Illescas, D. (Octubre de 2009). *creandoconciencia*. Available at creandoconciencia: http://creandoconciencia.org.ar/enciclopedia/accidentologia/modelos-fisicos-matematicos/SIMULACION-DE-CHOQUE-FRONTAL.pdf

Ingemecanica. (02 de 2020). *Ingemecanica*. Available at Ingemecanica: https://ingemecanica.com/tutorialsemanal/tutorialn218.html

Irausquín, I. (2012). *Universidad Carlos II de Madrid.* Available at Universidad Carlos II de Madrid: https://core.ac.uk/download/pdf/29403142.pdf

Matolcsy, M. (1996). Crassworthiness of bus structures and rollover protection. *Advance science institutes series*, 327.

Mohd, A., Noor, A., Muhammad, H., & Valliyappan, D. (2018). *International Journal of Engineering & Technology.* Available at International Journal of Engineering & Technology: https://www.sciencepubco.com/index.php/ijet/article/view/21897/10573